Cell Transplantation
2019, Vol. 28(8) 985–1001

DOI: 10.1177/0963689719834873
journals.sagepub.com/home/cll
SAGE

Sodium/Hydrogen Exchanger 1 Participates in Early Brain Injury after Subarachnoid Hemorrhage both *in vivo* and *in vitro* via Promoting Neuronal Apoptosis

Huangcheng Song[1,2*], Shuai Yuan[1*], Zhuwei Zhang[1], Juyi Zhang[1], Peng Zhang[1], Jie Cao[1,3], Haiying Li[1], Xiang Li[1], Haitao Shen[1], Zhong Wang[1], and Gang Chen[1]

Abstract

Sodium/hydrogen exchanger 1 (NHE1) plays an essential role in maintaining intracellular pH (pHi) homeostasis in the central nervous system (CNS) under physiological conditions, and it is also associated with neuronal death and intracellular Na^+ and Ca^{2+} overload induced by cerebral ischemia. However, its roles and underlying mechanisms in early brain injury (EBI) induced by subarachnoid hemorrhage (SAH) have not been fully explored. In this research, a SAH model in adult male rat was established through injecting autologous arterial blood into prechiasmatic cistern. Meanwhile, primary cultured cortical neurons of rat treated with 5 μM oxygen hemoglobin (OxyHb) for 24 h were applied to mimic SAH *in vitro*. We find that the protein levels of NHE1 are significantly increased in brain tissues of rats after SAH. Downregulation of NHE1 by HOE642 (a specific chemical inhibitor of NHE1) and genetic-knockdown can effectively alleviate behavioral and cognitive dysfunction, brain edema, blood-brain barrier (BBB) injury, inflammatory reactions, oxidative stress, neurondegeneration, and neuronal apoptosis, all of which are involved in EBI following SAH. However, upregulation of NHE1 by genetic-overexpression can produce opposite effects. Additionally, inhibiting NHE1 significantly attenuates OxyHb-induced neuronal apoptosis *in vitro* and reduces interaction of NHE1 and CHP1 both *in vivo* and *in vitro*. Collectively, we can conclude that NHE1 participates in EBI induced by SAH through mediating inflammation, oxidative stress, behavioral and cognitive dysfunction, BBB injury, brain edema, and promoting neuronal degeneration and apoptosis.

Keywords

subarachnoid hemorrhage, early brain injury, sodium/hydrogen exchanger 1, neuronal apoptosis

Introduction

Spontaneous subarachnoid hemorrhage (SAH) is a complex cerebrovascular disease with high rates of mortality and morbidity and poor clinical outcomes. It accounts for approximately 5% of all types of stroke, and causes nearly 25% of all cerebrovascular deaths[1,2]. Aneurysm rupture is the major cause of SAH (nearly 85% of cases of spontaneous SAH), and approximately 12% patients die before receiving medical attention, 33% within 48 h and 50% within 30 days after initial hemorrhage[3–5]. Despite the improvements achieved in the treatment and management of SAH patients, the prognosis is still not satisfactory[6–11]. Historically, many research studies have focused mainly on therapy targeted cerebral vasospasm (CVS) after SAH, but the clinical outcomes are unsatisfactory, and they fail to decrease the

[1] Department of Neurosurgery and Brain and Nerve Research Laboratory, The First Affiliated Hospital of Soochow University, Suzhou, Jiangsu Province, China
[2] Department of Neurosurgery, Haimen People's Hospital, Jiangsu Province, China
[3] Department of Neurosurgery, The First People's Hospital of Changzhou, Jiangsu Province, China
* Both the authors contributed equally to this article.

Submitted: July 6, 2018. Revised: December 14, 2018. Accepted: February 6, 2019.

Corresponding Authors:
Zhong Wang and Haitao Shen, Department of Neurosurgery and Brain and Nerve Research Laboratory, The First Affiliated Hospital of Soochow University, 188 Shizi Street, Suzhou, Jiangsu Province 215006, China.
Emails: dagezi120@126.com; shenhaitao1990@suda.edu.cn

incidence of delayed cerebral ischemia and mortality[3,12–14]. Lately, investigators have found that the early brain injury (EBI) induced by SAH may be a key factor affecting the prognosis of patients[1,15–18]. EBI occurs within first 72 h of the SAH, and contains a series of pathophysiological events, such as cerebral edema, blood-brain barrier (BBB) disruption, oxidative stress, inflammatory responses, excitotoxicity, and impaired ionic homeostasis[19]. In addition, an increasing number of studies have shown that neuronal apoptosis plays an essential role in EBI induced by SAH; however, the underlying mechanisms have not been fully illustrated[20,21].

The sodium/hydrogen exchangers (NHEs) are a family of membrane proteins that play an essential role in maintaining intracellular pH (pHi) homeostasis by mediating the electroneutral translocation of extracellular Na^+ for intracellular H^+[22,23]. The NHE family includes nine members (NHE1–NHE9) and a cluster of distantly NHE-related genes: NHA1 and NHA2[24]. NHE1 is distributed very broadly in the central nervous system (CNS) of mammals[25]. NHE1 can be activated by multiple stimulations, such as growth factors and hormones, osmotic shrinkage, mechanical stress, intracellular acidification, and hypoxia[26]. The activity of NHE1 is also regulated by various signals and proteins, such as calcineurin-like EF hand protein 1 (CHP1)[27–29]. Recently, the roles and underlying mechanisms of NHE1 in the CNS have attracted increasing attention. NHE1 plays an important role in pHi regulation in several CNS cells, such as cortical and hippocampal astrocytes, cortical neurons, and microglia[25,30,31]. Previous research suggests that pharmacological blockade of NHE1 by HOE 642 and genetic knockdown of NHE1 expression level can both decrease oxygen and glucose deprivation (OGD)/reoxygenation (REOX)-induced neuronal death and inhibit intracellular Na^+ and Ca^{2+} overload in primary cultured mouse cortical neurons[32]. Moreover, the nuclear translocation of apoptosis-inducing factor (AIF), the protein levels of activated-caspase 3, and the numbers of TUNEL-positive cells are obviously decreased in NHE1 heterozygous (NHE1+/−) mice following transient focal cerebral ischemia compared with those in wild-type mice[33]. However, the roles and the underlying mechanisms of NHE1 in SAH have not been reported.

Therefore, the relation between NHE1 and SAH was investigated in this research, particularly the role of the activity of NHE1 (regulated in combination with CHP1) in EBI, and the effect of NHE1 on neuronal apoptosis following SAH. We will explore the changes of protein levels of NHE1 and the interaction with CHP1 in brain tissues, and potential roles of NHE1 in EBI and neuronal apoptosis in both an *in vivo* and an *in vitro* model of SAH.

Materials and Methods

Ethics and Animals

All animal experimental protocols (including all use, care, and operative procedures) were approved by the Ethics Committee of the First Affiliated Hospital of Soochow University and were performed in accordance with the guidelines of the National Institutes of Health on the care and use of animals. All animal experiments complied with the Animal Research: Reporting of In Vivo Experiments (ARRIVE) guidelines. In this study, adult male Sprague-Dawley (SD) rats weighing 300–350 g were provided from the Animal Center of the Chinese Academy of Sciences (Shanghai, China), and were housed in temperature- and humidity-controlled animal quarters with a 12 h light/dark cycle; food and water were provided without restriction. Every effort was made to minimize the numbers of animals used and their suffering.

Establishing the SAH Model in vivo

As reported in our previous study[34], an experimental SAH model in rats induced by the injection of autologous arterial blood into the prechiasmatic cistern was used in this research. Briefly, after intraperitoneally anesthesia with 4% chloral hydrate, the rats were fixed in the stereotaxic apparatus. Additionally, rectal temperature was maintained at 37 ± 0.5°C by a feedback-controlled heating pad. The right femoral artery was catheterized to monitor arterial blood pressure and blood glucose levels. Next, a needle was inserted stereotaxically into the prechiasmatic cistern of each rat. The needle was inserted 7.5 mm anterior to bregma in the midline, and the final position of the needle tip was 2–3 mm anterior to the chiasma and retracted 0.5 mm. Subsequently, 300 µl autologous arterial blood collected from the femoral artery was injected into the prechiasmatic cistern by using an aseptic syringe pump. In the Sham group in this study, rats were injected with 300 µl physiological saline solution. After SAH model induction, the rats were immediately injected with 5 ml 0.9% saline to avoid dehydration. Following recovery for 1 h, all rats were returned to the cages, and room temperature was maintained at 22–24°C. It could be observed that the inferior basal temporal lobe of brain was obviously stained by blood (Fig. 1A). Subsequently, the rats were euthanized at the indicated time points following SAH induction, and brain tissues surrounding the hemorrhage were obtained and used in further experiments. The temporal base brain tissues were applied mainly to Western blot and immunoprecipitation analysis, and the total coronal sections containing temporal base brain tissues were subjected to immunofluorescence, TUNEL, Nissl and FJB staining. A schematic representation of brain tissues and their application to subsequent assay is shown in Fig. 1A.

Induction of the SAH Model in vitro

As described in previous research[35], cortical tissues were collected from the fetal rats at 18 days of gestation to create primary neuron-enriched cultures. Firstly, meninges and blood vessels were removed from cerebral hemispheres. Secondly, 0.25% trypsin (GIBCO, Grand Island, NY, USA)

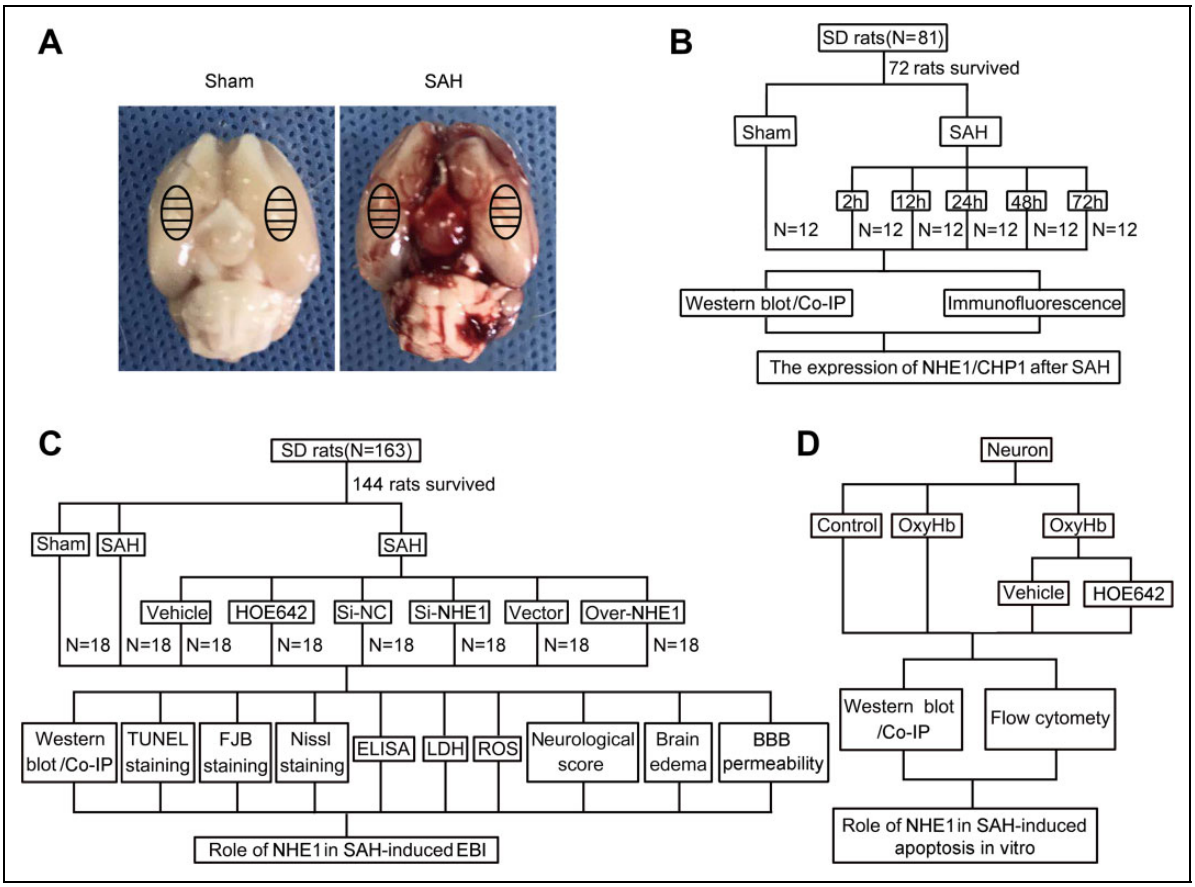

Fig. 1. Subarachnoid hemorrhage (SAH) model and experimental design. (A) Schematic representation of brain tissues of rats (Sham and SAH group) that were applied for further experiments. (B) Experiment 1 was designed to assess protein levels of NHE1 in brain tissues of rats after SAH at various time points. (C) Experiment 2 was designed to evaluate effects of NHE1 on early brain injury (EBI) induced by SAH. (D) Experiment 3 was designed to elucidate the role of the NHE1 in neuronal apoptosis induced by SAH *in vitro*.

was used to digest brain tissues for 5 min at 37°C; digestion was terminated through washing brain tissues three times with PBS. The suspension of brain tissues was then centrifuged at 1000 *g* for 5 min, and the pellet resuspended in complete medium (Neurobasal medium with 2% B27, 0.5 mM GlutaMAX TM-I, 50 U/ml penicillin, and 50 U/ml streptomycin; all from GIBCO). Lastly, the neurons were plated at a density of 20,000 cells/cm^2 into 6-well plates (Corning, Corning, NY, USA) precoated with 0.1 mg/ml poly-D-lysine (Sigma-Aldrich, St. Louis, MO, USA) and cultured in complete medium. The primary cultured neurons were maintained at 37°C under humidified conditions and 5% CO_2 for 10–14 days. Half the medium volume was exchanged every 2 days. To mimic SAH, the cultured neurons were treated with 5 μM oxygen hemoglobin (OxyHb) for 24 h at 37°C.

Experimental Design

Before the SAH model was established, all rats were numbered and divided randomly, using a table of random numbers, into two groups (30 rats in the Sham group and the others in the SAH group) by a researcher who is entirely blind to the experimental groups. After SAH induction, all SAH rats were divided randomly into several groups (particulars as follows) by the same researcher, also using a table of random numbers. In experiment 1, 72 rats (12 rats come from the Sham group; and 60 rats surviving after surgery from an initial 69 rats in the SAH group) were assigned randomly to six groups (12 rats per group): a Sham group and five experimental groups ordered by time points: 2, 12, 24, 48, and 72 h following SAH induction. At the indicated time points after SAH induction, all rats were anaesthetized by chloral hydrate, and their cerebral tissues were collected for subsequent analysis after transcardial perfusion with PBS. In each group, partial underlying temporal base brain tissues of six rats were frozen in liquid nitrogen for Western blot and immunoprecipitation analyses, and total coronal sections containing temporal base tissues of the other six rats were subjected to immunofluorescence analysis (Fig. 1B). In experiment 2, 144 rats (18 rats from Sham group; and 126 rats surviving after surgery, from an initial 145 rats in the SAH group) were divided randomly into eight groups

(18 rats in each group): Sham group, SAH group, SAH + Vehicle group, SAH + HOE642 group, SAH + Negative Control SiRNA (Si-NC) group, and SAH + NHE1 SiRNA (Si-NHE1) group, SAH + Vector group, and SAH + NHE1 overexpression (Over-NHE1) group. In each group, 18 rats were divided randomly using a table of random numbers into three subgroups by a researcher who did not participate in this study. For six rats, total coronal sections containing temporal base tissues were obtained for immunofluorescence, FJB, Nissl, and TUNEL stainings. The underlying temporal base brain tissues of the other six rats were collected and used in Western blot analysis, immunoprecipitation analysis, reactive oxygen species (ROS) assay, and BBB permeability. The last six rats in each group were sacrificed for brain edema test (Fig. 1C). In brain edema and behavioral impairment tests, the researcher is entirely blinded to the experimental groups. For quantitative analyses in Western blot analysis, immunoprecipitation analysis, ROS assay, and BBB permeability, each "*n*" represents individual data obtained from one independent experiment using one rat, and combined data come from at least six independent experiments from six different rats. In experiment 3, HOE642 was used to test the effects of NHE1 in neuronal apoptosis *in vitro* (Fig. 1D). Primary cortical neurons were divided into four groups for Western blot and immunoprecipitation analyses, and Annexin V and PI staining as below: Control group, OxyHb group, OxyHb + Vehicle group, and OxyHb + HOE642 group; "*n*" was defined as the number of independent experiments in every figure legend.

Transfection of Plasmids and siRNA in Rats

Plasmids and SiRNA transfections in rats are performed as previously described[36]. Briefly, 5 μg NHE1 overexpression plasmid and 5 μg Vector plasmid (NHE1 Gene ID: 24782; both from GenScript, Nanjing, China) were each dissolved in 5 μl endotoxin-free water. Next, 10 μl Entranster-*in vivo* DNA transfection reagent (Engreen, Beijing, China) was immediately added to 5 μl plasmid solution, and mixed for another 15 min. Finally, 15 μl of this mixture was injected intracerebroventricularly under the guidance of a stereotaxic apparatus after anesthesia. On the other hand, NHE1 SiRNA and Negative Control SiRNA (both from RIBOBIO, Guangzhou, China) were dissolved in 5 μl RNase-free H_2O to a final concentration of 100 pmol/μl, then added to 10 μl transfection reagent (Entranster-*in vivo* RNA transfection, Engreen, Beijing, China) and mixed gently for another 15 min. Finally, this 15 μl mixture was also injected intracerebroventricularly to rats. The puncture point of lateral ventricle was located at 1.5 mm posterior, 1.0 mm lateral, and 3.2 mm below the horizontal plane of bregma. At 24 h after these processes, the SAH model of rats is established.

Drug Administration

Based on a former study, the HOE642 (also called as cariporide, a specific inhibitor of NHE1, Sigma-Aldrich) was injected intravenously in rats at a dose of 15 mg/kg at 20 min before induction of SAH[37]. The HOE642 is dissolved in DMSO, and then diluted in 0.9% saline according to its final concentration. Additionally, in the *in vitro* experiment, the final concentration of HOE642 was 1 μM in the medium. The culture neurons were pretreated with HOE642 at 37°C for 2 h, then thorough rinsed with PBS, fresh complete medium was added and incubated with OxyHb (5 μM) for another 24 h at 37°C[38].

Western Blot Analysis

As described in our previous study[39], all brain tissue samples were lysed in a lysis buffer containing phenylmethylsulfonyl fluoride (PMSF), and then an enhanced bicinchoninic acid (BCA) protein assay kit (all from Beyotime, Shanghai, China) was applied to detect protein concentrations of each brain tissue sample. Molecular weight markers (Thermo Fisher Scientific, Waltham, MA, USA) and protein samples (30 μg/lane) were loaded on a 10% SDS-polyacrylamide gel, separated, and then transferred electrophoretically to a polyvinylidene difluoride (PVDF) membrane (Merck Millipore, Billerica, MA, USA). The membrane was blocked with 5% bovine serum albumin (BSA, BIOSHARP, Hefei, China) at 37°C for 1 h. Subsequently, the membrane was incubated with primary antibodies at 4°C overnight. The primary antibodies against NHE1 and CHP1 (both purchased from Santa Cruz Biotechnology, Santa Cruz, CA, USA) were diluted 1:1000 before incubating. The primary antibody against β-actin diluted 1:5000 served as a loading control. The membrane was incubated with appropriate horseradish peroxidase (HRP)-linked secondary antibody (Santa Cruz Biotechnology) at 37°C for 1 h, and subsequently washed with PBST (PBS + 0.1% Tween 20) three times. Finally, an enhanced chemiluminescence kit (Thermo Fisher Scientific) was applied to signal detection. The quantity of protein was analyzed with the program Image J (National Institutes of Health, Bethesda, MD, USA) and normalized to that of loading controls.

Immunoprecipitation Analysis

As mentioned in a previous report[40], briefly, brain tissue samples and cultured neurons were mechanically lysed in a lysis buffer with PMSF (both from Beyotime). Next, specific antibody (against CHP1) or normal rabbit IgG (both from Santa Cruz Biotechnology) were applied and the lysate was incubated overnight at 4°C with agitation. The protein A + G Sepharose beads were then added respectively to immune complex and these lysate-bead mixture were incubated at 4°C for 4 h with rotary agitation. SDS-PAGE and

immunoblotting were subsequently performed to allow protein separation and detection.

Immunofluorescence Microscopy

Immunofluorescence analysis was performed as previously mentioned[41]. Total coronal sections with temporal base tissues (thickness 4 μm) were used for immunofluorescence analysis in this study. After antigen retrieval and non-specific-binding blocking, brain sections were incubated with primary antibodies against NHE1, CHP1, and the NeuN-neuronal marker (the former two antibodies come from Santa Cruz Biotechnology and the latter from Abcam, Cambridge, MA, USA, 1:300 dilution) at 4°C overnight. Next, these brain sections were washed three times with PBST (PBS + 0.1%Tween 20) and incubated with suitable secondary antibodies (Life Technologies, Gaithersburg, MD, USA, 1:500 dilution) for 1 h at 37°C. Subsequently, these sections were washed three times using PBST and coverslipped with mounting medium containing 4,6-diamino-2-phenylindole (DAPI, SouthernBiotech, Birmingham, AL, USA). Finally, a fluorescence microscope (Olympus BX50/BX-FLA/DP70, Olympus Co., Tokyo, Japan) was applied to observe brain sections, and these sections were observed by a researcher who is entirely blind to experimental conditions. The Image J program (National Institutes of Health, Bethesda, MD, USA) was used to analyze relative fluorescence intensity in each photomicrograph. At least three photomicrographs from each brain section were obtained, and one section from each rat was used to perform this experiment. One photomicrograph from each rat in each group was used in quantitative analysis.

TUNEL and FJB Staining

Terminal deoxynucleotidyl transferase–mediated dUTP nick-end labeling (TUNEL) staining was used to measure apoptosis in brain tissues of rats in various groups based on the manufacturer's protocol (Roche, Basel, Switzerland). Firstly, stained slides were incubated with the TUNEL reaction mixture at 37°C for 1 h, and then with NeuN-neuronal markers (Abcam, 1:300 dilution) at 4°C overnight. Next, a suitable secondary antibody (Life Technologies) was incubated with the brain sections. The degree of neuronal apoptosis was visualized by a fluorescence microscope (Olympus BX50/BX-FLA/DP70, Olympus Co.). TUNEL-positive neurons were counted by a researcher blind to the experimental conditions. Neuronal apoptosis was defined as the average number of TUNEL-positive neurons in each brain section from each rat.

As mentioned in our previous research[42], neurodegeneration in brain tissues of rats following SAH is detected by Fluoro-Jade B (FJB) staining. After deparaffinization and rehydration, brain sections are incubated successively in 80% alcohol with 1% NaOH for 5 min, 70% alcohol for 2 min, 0.06% potassium permanganate for 10 min, and 0.0004% FJB working solution for 30 min. Subsequently, brain sections were washed and dried for 10 min in an incubator (50–60°C). Finally, these brain sections are cleared in xylene and coversliped by using a mounting medium (Distyrene Plasticiser Xylene, Sigma-Aldrich). These sections were observed by a researcher who is entirely blind to experimental conditions.

Nissl Staining

Nissl staining was applied to measure neuronal loss in brain tissues as mentioned in a previous study[35]. After being deparaffinized and hydrated to distilled water, the brain sections were incubated with 0.5% toluidine blue at 37°C for 30 min, and were then dehydrated with graded alcohols and cleared in xylene. Finally, these sections were coverslipped using neutral resins and observed in a light microscope by a researcher entirely blind to experimental conditions. We obtained at least three photomicrographs per section in the temporal cortex near the blood clot, and at least one brain section was subjected to this staining in each rat. In quantitative analysis, at least one photomicrograph was taken in each rat from each group. The surviving neurons with pale nuclei and large cellular bodies were counted and averaged; dark stained neurons and shrunken cellular bodies were considered dead and excluded from Nissl counting. The quantitative data are shown as numbers of surviving neurons per field in each brain section.

Enzyme-Linked Immunosorbent Assay (ELISA)

The levels of TNF-α and IL-1β in cerebro-spinal fluid (CSF) of rats in each group were measured using specific ELISA kits (eBioscience, San Diego, CA, USA) based on the manufacturer's instructions.

ROS Assay

The levels of ROS were measured using a Reactive Oxygen Species Assay Kit (KeyGEN BioTECH, Nanjing, China) in brain tissues of rats in experiment 2, and served as a measure of the relative levels of oxidative stress. The collected brain tissues were mechanically lysed in a lysis buffer, and then centrifuged at 12,000 *g* at 4°C for 10 min. The supernatants were obtained and applied to the ROS assay. ROS levels were measured by using the oxidant-sensitive probe 2,7-dichlorofluorescein diacetate (DCF-DA) based on the manfacturer's instructions. A fluorometric microplate reader (FilterMax F5, Molecular Devices, Eugene, OR, USA) was used to test the fluorescence intensity of each sample, and all samples were measured in at least one dependent experiment. The concentrations of ROS are shown as fluorescence intensity/

Table 1. Neurobehavioral Evaluation.

Category	Behavior	Score
Appetite	Finished meal	0
	Left meal unfinished	1
	Scarcely ate	2
Activity	Walk and reach at least three corners of the cage	0
	Walk with some stimulations	1
	Almost always lying down	2
Deficits	No deficits	0
	Unstable walk	1
	Impossible to walk	2

mg total protein, and the data of all groups were normalized to those of the Sham group.

Neurological Impairment

At 24 h after SAH, all rats were examined for behavioral impairment using a published scoring system, and monitored for appetite, activity, and neurologic defects in experiment 2 (details shown in Table 1)[39]; the behavior and activity score of each rat was evaluated by a technician who did not know to which group each rat belonged.

Brain Edema

The wet/dry weight method was applied to detect the level of brain edema as mentioned previously[34]. At 24 h after SAH, six rats in each group in experiment 2 were anesthetized and their brain tissues collected. After removing the brainstem and cerebellum, the brain samples were weighed immediately (recorded as wet weight), and then dried at 100°C for 72 h. Next, they were weighed again to obtain dry weight. The percentage of brain water content in each sample was calculated by: [(wet weight−dry weight)/wet weight] × 100%.

BBB Injury

BBB disruption of rats induced by SAH was measured by the level of albumin extravasation[43]. Generally, due to the existence of the BBB, the level of albumin in brain tissues is tiny. However, the BBB is destroyed following SAH; albumin protein levels in brain tissues would be obviously increased. Thus, changes in albumin levels could serve as an indicator of BBB injury. Western blot analysis was applied to detect the levels of albumin in brain tissues of rats in various groups. In brief, brain tissues were mechanically lysed in a lysis buffer containing phenylmethylsulfonyl fluoride (PMSF), and the protein concentration of each brain tissue samples was measured by the bicinchoninic acid (BCA) method (enhanced BCA protein assay kit, all from Beyotime). Molecular weight markers (Thermo Fisher Scientific) and protein samples (30 μg/lane) were loaded onto a 10% SDS-polyacrylamide gel, separated, and transferred electrophoretically to a PVDF membrane (Merck Millipore, Billerica, MA, USA), which was subsequently blocked with 5% BSA at 37°C for 1 h. The membrane was then incubated at 4°C overnight with primary antibodies. The primary antibody against albumin (Abcam) was diluted 1:5000; and the primary antibody against β-actin served as a loading control. Subsequently, the membrane was incubated with a suitable HRP-linked secondary antibody (Santa Cruz Biotechnology, Santa Cruz, CA, USA) at 37°C for 1 h and then washed three times with PBST (PBS + 0.1% Tween 20). Finally, an enhanced chemiluminescence kit (Thermo Fisher Scientific) was applied to signal detection. The quantitative analysis of protein levels of albumin was performed with the Image J program (National Institutes of Health) and normalized to that of loading controls.

Annexin V and PI Staining in vitro

As our previous study described[40], neuronal apoptosis is detected by Annexin V and PI staining in vitro. After treatments, the primary cultured neurons were trypsinized using 0.25% trypsin (without EDTA, GIBCO, Grand Island, NY, USA), and then centrifuged at 300 *g* for 5 min. The cell pellet was resuspended in 500 μl binding buffer and then mixed with 5 μl Annexin V and 5 μl PI (Beyotime, Shanghai, China). Ultimately, after incubation at 37°C for 20 min, the neuron samples were analyzed by flow cytometry (FACS Calibur, BD, San Jose, CA, USA), and at least 50,000 events in each sample were recorded.

Statistical Analysis

In this research, all data are shown as mean ± SEM. SPSS 11.5 (SPSS Inc., Armonk, NY, USA) was applied for statistical analyses. Before performing statistical analysis, the data sets were tested for normality of distribution in each group by Kolmogorov-Smirnov test. The data groups (two groups) with normal distribution were compared with two-sided unpaired Student's *t*-test, and the Mann-Whitney U-test was applied for nonparametric data. $p < 0.05$ was considered statistically significant. The sample sizes are determined by power analysis during the animal ethics dossier application in this study; and the power analysis of each two-sided unpaired Student's *t*-test or Mann-Whitney U-test was performed by SAS 9.0 (SAS Institute Inc., Cary, NC, USA); all power analysis in this research was > 0.8.

Results

General Observation

No significant difference was observed in body temperature, body weight, blood gas, and mean arterial blood pressure of rats in any of the SAH experimental groups (data not shown). No animals died (0/30 rats) in the Sham group, and the

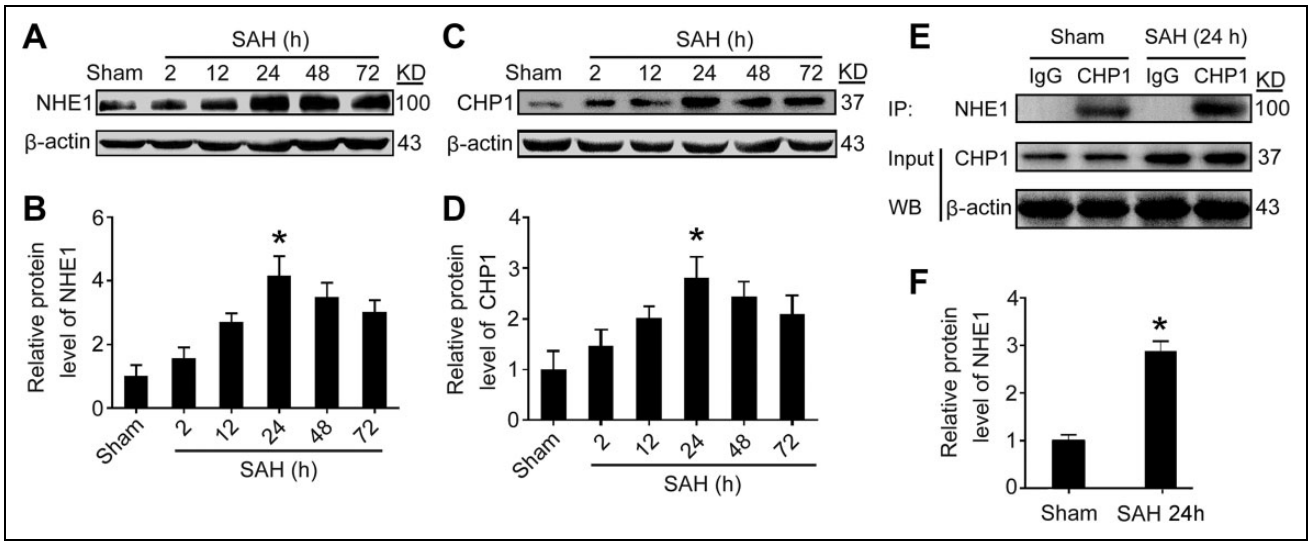

Fig. 2. Protein levels of NHE1 and CHP1 in brain tissues of rats after SAH. (A) Western blot analysis reveals the protein levels of NHE1 in brain tissues at various time points. (B) Quantification of protein levels of NHE1 at various time points. (C) Protein levels of CHP1 in brain tissues of rats after SAH is detected. (D) Quantification of protein levels of CHP1 at various time points. (E) The interaction of NHE1 and CHP1 in brain tissues of rats at 24 h after SAH was also tested through immunoprecipitation (IP) analysis. Input, 5% of extract before IP. (F) Quantification of protein levels of NHE1 interacted with CHP1 in brain tissues at 24 h after SAH. In (B), (D) and (F), all data are shown as mean ± SEM. Mean values of Sham group were normalized to 1.0. *$p < 0.05$ vs. Sham group; $n = 6$.

mortality rate of the rats after SAH induction was 13% (28/214 rats).

Protein Levels of NHE1 are Increased in Brain Tissues of Rats After SAH Induction

To detect the protein levels of NHE1 in rat brain tissues at various time points following SAH induction, Western blot analysis of temporal base brain tissues and double immunofluorescence of brain sections were performed. The results of Western blot analysis suggest that SAH caused significantly increasing in levels of NHE1 compared with that in the Sham group. After SAH induction, protein levels of NHE1 increased gradually, peaked at 24 h, and then subsequently decreased sharply ($p < 0.05$, Fig. 2A, B). We also detected protein levels of CHP1 in brain tissues after SAH; the results of Western blot analysis show that the levels of CHP1 are upregulated and peaked at 24 h after SAH ($p < 0.05$, Fig. 2C, D). To further evaluate the interaction of NHE1 and CHP1, immunoprecipitation (IP) was applied in this study. The results of IP suggest that the interaction of NHE1 and CHP1 is significantly increased in the brain tissues of rats after SAH ($p < 0.05$, Fig. 2E, F). Double immunofluorescence assay was also used to confirm the increasing of levels of NHE1 and CHP1 protein in brain tissues after SAH. The results of immunofluorescence staining show a similar trend as the Western blots in the levels of NHE1 and CHP1 in brain tissues after SAH (Fig. 3A–C).

Inhibiting NHE1 by Chemical Inhibitor and Genetic-Knockdown Alleviates Brain Injury in Rats After SAH

To determine whether NHE1 is involved in EBI after SAH, a specific chemical inhibitor of NHE1, HOE642, was applied in this research. Moreover, treatment with genetic-knockdown by SiRNA interference (SiRNA-NHE1), and overexpression of NHE1 from a recombinant plasmid (Over-NHE1) were also used in SAH rats. The results of Western blot analysis and double-immunofluorescence staining suggest that the treatments with HOE642 and SiRNA-NHE1 transfection could significantly reduce NHE1 protein levels, but recombinant plasmid transfection can obviously increase the protein levels of NHE1 in brain tissues of rats after SAH (all $p < 0.05$, Fig 4A, B and Fig 5A, B). The results of IP show that the interaction of NHE1 and CHP1 is significantly inhibited by treatments with HOE642 and SiRNA-NHE1 transfection, while it is increased markedly using recombinant plasmid transfection in brain tissues after SAH (all $p < 0.05$, Fig 4C, D).

The levels of IL-1β and TNF-α in the CSF of rats in various groups were measured by ELISA. The results indicate that the levels of IL-1β and TNF-α were significantly decreased by HOE642 and SiRNA-NHE1 treatment compared with those in SAH + Vehicle group and SAH + Si-NC group, respectively; but they are obviously increased in the SAH + Over-NHE1 group compared with those in the SAH + Vector group. These results suggest that inhibiting NHE1 improves symptoms of inflammation in brain tissues of SAH rats (all $p < 0.05$, Fig 6A). In addition, the levels of ROS, an indicator of oxidative stress, and lactate

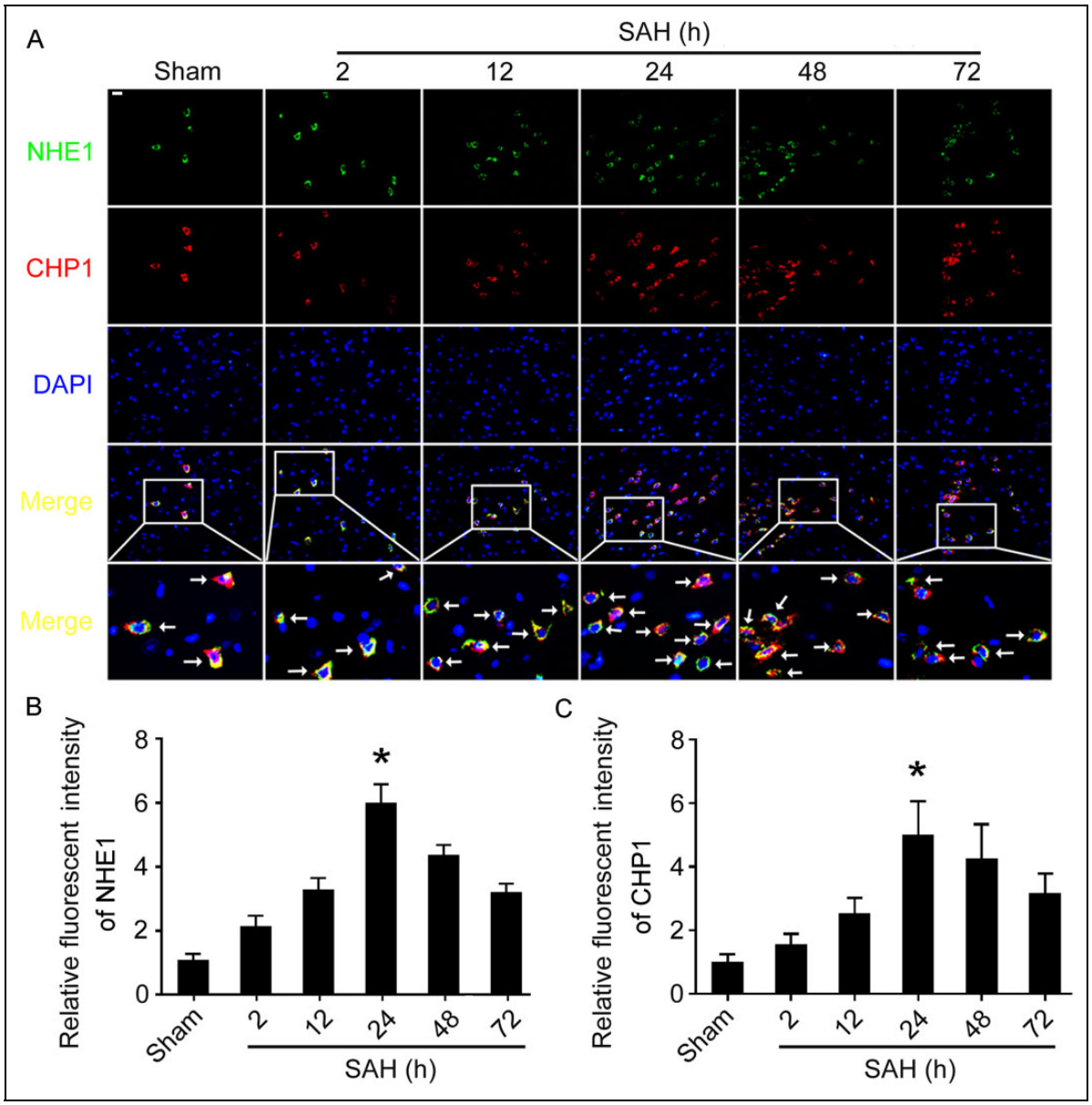

Fig. 3. (A) Double immunofluorescence is performed in brain sections using antibodies for NHE1 (green) and CHP1 (red). Nuclei are fluorescently labeled by DAPI (blue). Arrows indicate NHE1- and CHP1- positive cells. Scale bar = 20 μm. Relative fluorescence intensities of NHE1 (B) and CHP1 (C) in brain sections are also shown. In (B) and (C), all data are shown as mean ± SEM. Mean values of Sham group are normalized to 1.0. *$p < 0.05$ vs. Sham group; $n = 6$.

dehydrogenase (LDH), an index of necrosis, were also tested in this study. The results show that the levels of ROS and LDH are both clearly reduced in the SAH + HOE642 and SAH + Si-NHE1 groups compared with those in the SAH + Vehicle and SAH + Si-NC groups, respectively; while they are increased markedly following Over-NHE1 treatment compared with those in the SAH + Vector group. These results indicate that inhibiting NHE1 alleviates oxidative stress and necrosis in brain tissues of rats induced by SAH (all $p < 0.05$, Fig 6B and E). The results of Nissl staining show that there are more surviving neurons in the temporal cortex of SAH rats after HOE642 and Si-NHE1 treatments than those in the SAH + Vehicle and SAH + Si-NC groups, respectively; however, surviving neurons are significantly reduced in the SAH + Over-NHE1 group compared with those in the SAH + Vector group. These results demonstrate that inhibiting NHE1 can reduce neuronal loss in brain tissues of rats following SAH induction (all $p < 0.05$, Fig 6C, D).

In this research, BBB permeability was detected by albumin extravasation, and Western blot analysis was applied to test albumin protein levels in brain tissues of rats in each

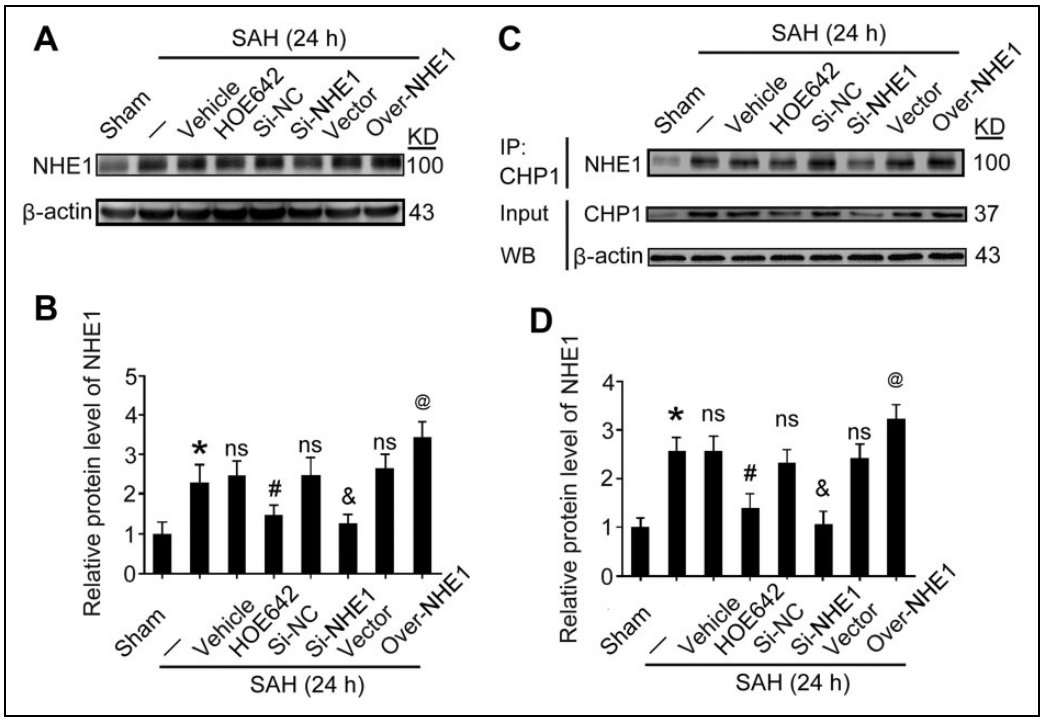

Fig. 4. Different effects of chemical inhibitor, genetic-knockdown and - overexpression on the protein levels of NHE1 in brain tissues of rats at 24 h after SAH. (A) Western blot analysis show that the protein levels of NHE1 were significantly decreased in HOE642 and Si-NHE1 treatment groups, whereas levels increased in the SAH + Over-NHE1 group. (B) Quantification of relative protein levels of NHE1 in various groups are shown. (C) The interactions of NHE1 and CHP1 in brain tissues of rats at each group were also tested by IP analysis. Input, 5% of extract before IP. (D) Quantification of protein levels of NHE1 interacted with CHP1 at various groups. All data are presented as mean ± SEM; $^{*}p < 0.05$ compared with Sham group; ns, no significant difference vs. SAH group; $^{\#}p < 0.05$ vs. SAH + Vehicle group; $^{\&}p < 0.05$ vs. SAH + Si-NC group; $^{@}p < 0.05$ vs. SAH + Vector group; $n = 6$.

group; the results suggest that treatment with HOE642 and Si-NHE1 significantly inhibit albumin extravasation and BBB injury in rats induced by SAH, while protein levels of albumin increased markedly after Over-NHE1 treatment compared with those in the SAH + Vector group (all $p < 0.05$, Fig 7A, B). Brain water content was evaluated by the wet and dry weight method. The results show that brain water content was obviously inhibited in the SAH + HOE642 and SAH + Si-NHE1 groups compared with those in SAH + Vehicle and SAH + Si-NC groups, respectively, while brain water content increased markedly following Over-NHE1 treatment compared with brain water content in the SAH + Vector group (all $p < 0.05$, Fig 7C). The neurological scores of rats in SAH + HOE642 and SAH + Si-NHE1 groups were obviously lower than those in the SAH + Vehicle and SAH + Si-NC groups, respectively; however, the neurological score of rats were significantly higher in the SAH + Over-NHE1 group than those in the SAH + Vector group (all $p < 0.05$, Fig 7D). These results suggest that NHE1 participates in EBI after SAH, including inflammation, oxidative stress, neuronal loss, BBB injury, brain edema, and neuronal dysfunction.

Increased NHE1 Promotes Neuronal Apoptosis and Degeneration in Brain Tissues of Rats Following SAH

We performed FJB and TUNEL staining to evaluate the roles of NHE1 in neuronal degeneration and apoptosis, respectively, in brain tissues of rats in various groups. There were significant increases in the ratios of cell apoptosis and neuronal degeneration in brain tissues of rats in the SAH group compared with those in the Sham group. Meanwhile, inhibition of NHE1 by HOE642 treatment, and downregulation of NHE1 by Si-NHE1 treatment, can both decrease the cell apoptosis ratio, while more TUNEL-positive neurons were observed in brain tissues following overexpression of NHE1 (all $p < 0.05$, Fig. 8A, C). Results of FJB staining suggest that more neurodegenerative neurons exist in the cortex of rats in the SAH group compared with the Sham group. Inhibition of NHE1 by HOE642 and Si-NHE1 treatments can both reduce neuronal degeneration in the cortex of rats compared with the SAH + Vehicle group and SAH + Si-NC group, respectively. Upregulation of NHE1 markedly increased the numbers of neurodegenerative neurons in the cortex of rats, while there was no obvious effect in the SAH + Vector treatment group (all $p < 0.05$, Fig. 8B, D).

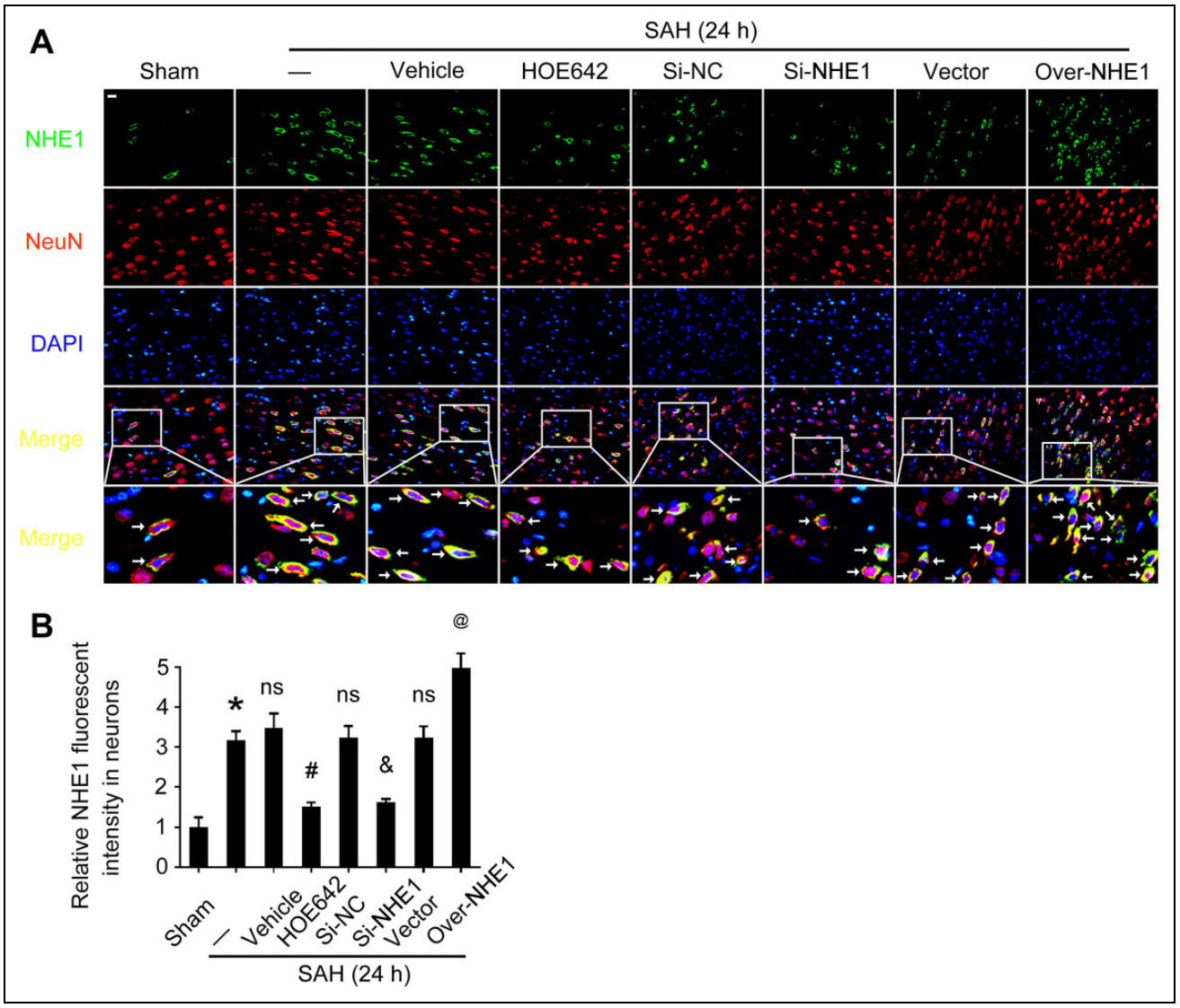

Fig. 5. (A) Double-immunofluorescence analysis was performed with antibodies against NHE1 (green) and NeuN (neuronal marker, red), and nuclei are fluorescently labeled by DAPI (blue). Arrows point to NHE1-positive neurons. Scale bar = 20 μm. (B) Quantification of the relative fluorescence intensity of NHE1 in brain tissues is shown. The mean fluorescence intensity of Sham group is normalized to 1.0. All data are shown as mean ± SEM; $^{*}p < 0.05$ compared with Sham group; ns, no significant difference vs. SAH group; $^{\#}p < 0.05$ vs. SAH + Vehicle group; $^{\&}p < 0.05$ vs. SAH + Si-NC group; $^{@}p < 0.05$ vs. SAH + Vector group; $n = 6$.

Inhibition of NHE1 Exerts Protective Effects on Apoptosis in Cultured Neurons Subjected to OxyHb Treatment

In vitro experiments confirmed that expression of NHE1 increased in cultured neurons subjected to OxyHb treatment compared with the Control group. Furthermore, OxyHb treatment increased the interaction of NHE1 and CHP1 in neurons, which could be attenuated when the neurons were treated with HOE642 (all $p < 0.05$, Fig. 9A, B). To identify the effects of NHE1 on neuronal apoptosis *in vitro*, Annexin V and PI staining was utilized in this experiment. The results of Annexin V and PI staining suggest that, compared with the Control group, more apoptotic cells were detected in the OxyHb group, while the ratio of apoptotic cells was markedly reduced by HOE642 treatment compared with the OxyHb + Vehicle group (all $p < 0.05$, Fig. 9C–J). These results indicate that inhibiting NHE1 by HOE642 treatment can significantly reduce OxyHb-induced apoptosis in neurons *in vitro*.

Discussion

Cell death plays an important role in EBI following SAH[1,16]. Previous research has reported that both apoptotic and necrotic cells exist in the brain tissues of patients with SAH and in experimental SAH animal models[44]. However, only a few reports note that necrosis contributes to EBI after SAH[45];

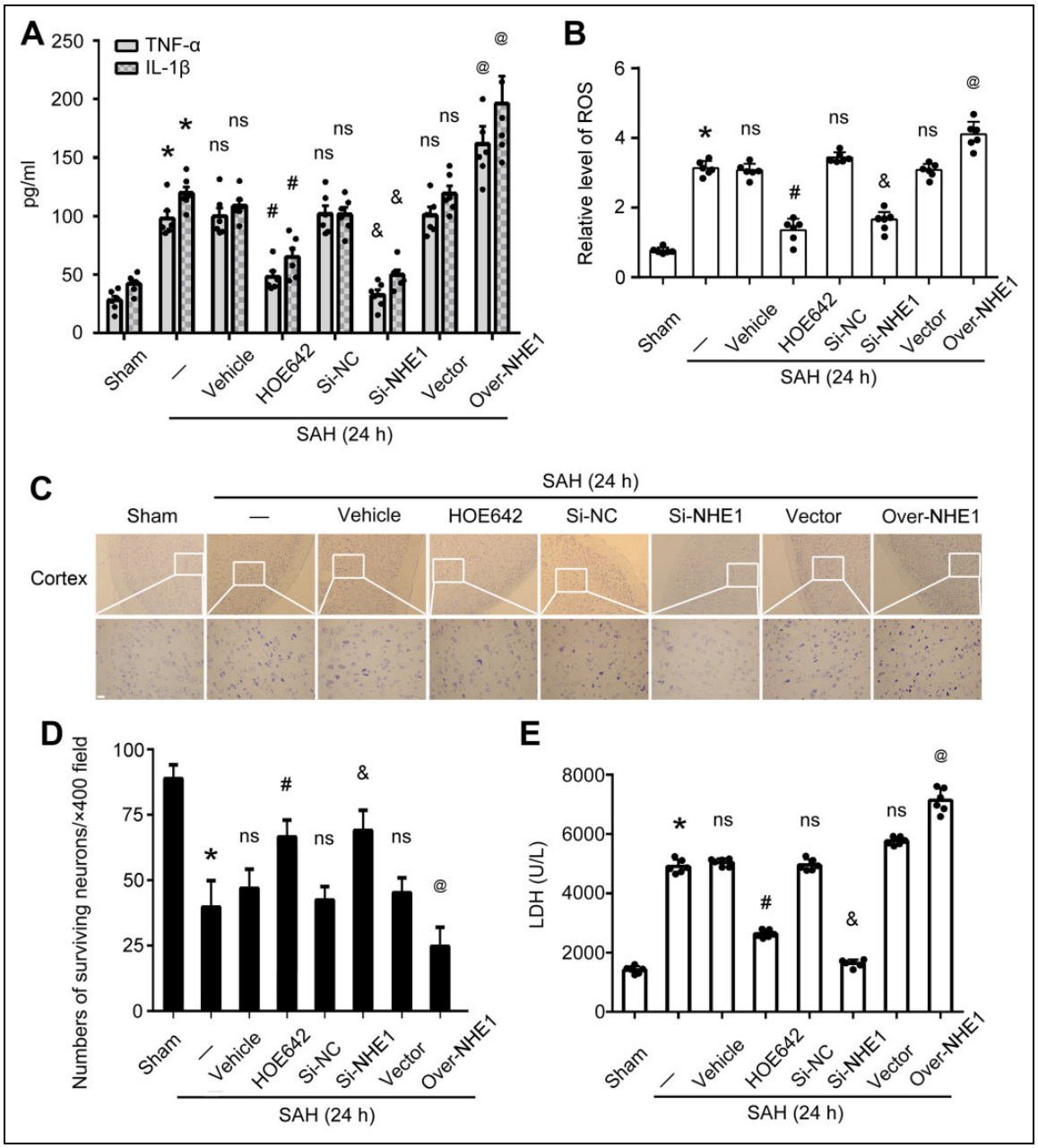

Fig. 6. Roles of NHE1 in EBI induced by SAH *in vivo*. Concentrations of TNF-α (A) and IL-1β (B) in cerebro-spinal fluid (CSF) of rats at various groups are shown. (B) Relative levels of reactive oxygen species (ROS) in brain tissues of rats at various groups. Mean values of Sham group are normalized to 1.0. (C) Nissl staining shows surviving neurons in the cortex of rats in each group. Scale bar = 20 μm. (D) Quantification of surviving neurons per ×400 field in the cortex of rats in various groups. (E) Relative levels of lactate dehydrogenase (LDH) in CSF of rats at various groups. Mean values of Sham group are normalized to 1.0. In (A), (B), (D) and (E), all data are presented as mean ± SEM; *$p < 0.05$ vs. Sham group; ns, no significant difference vs. SAH group; $^{\#}p < 0.05$ vs. SAH + Vehicle group; $^{\&}p < 0.05$ vs. SAH + Si-NC group; $^{@}p < 0.05$ vs. SAH + Vector group; $n = 6$.

almost all previous studies think that apoptosis is the major form of cell death in brain tissues after SAH, although the mechanisms have not been fully elucidated. Recently, NHE1—a membrane protein that plays an important role in maintaining intracellular pH (pHi) homeostasis in cells through the electro-neutral translocation of extracellular Na^+ for intracellular H^+—has attracted much attention[22,23]. It is reported that NHE1 participates in neuronal death in brain tissues induced by transient forebrain ischemia in a Mongolian gerbil model[46]. A previous study also showed that NHE1 contributes to neuronal death induced by OGD in primary cultured mouse neurons[32]. It has been proved that the intracellular acidosis induced by ischemia could trigger the excessive activation of NHE1, and result in intracellular

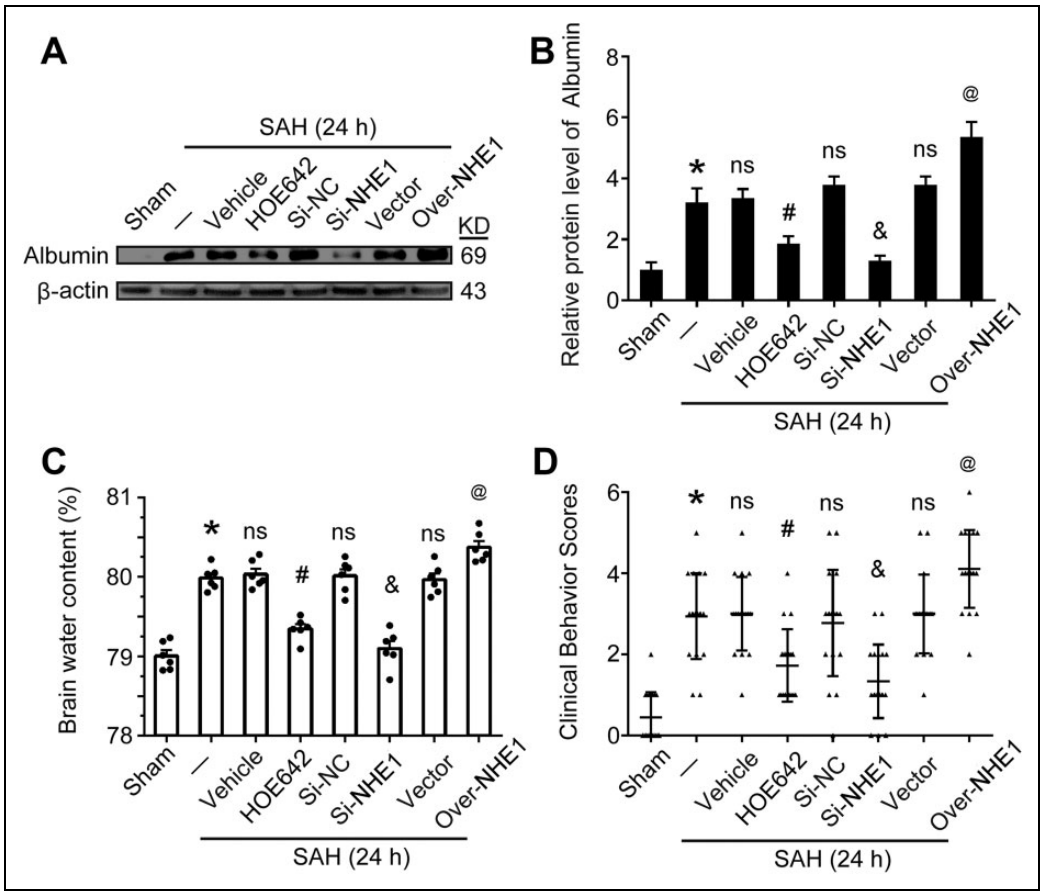

Fig. 7. Inhibiting NHE1 by chemical inhibitor and genetic-knockdown alleviates blood-brain barrier (BBB) injury, brain edema and neurological impairment in rats following SAH. (A) Western blot analysis measures the protein levels of albumin in brain tissues of rats in various groups. (B) Quantification of relative protein levels of albumin in various groups; mean values of Sham group are normalized to 1.0. (C) Bar graphs showed the effects of NHE1 on brain water content of rats in various groups. (D) The neurological scores in various groups are shown; data are shown as individual data. In (B), (C) and (D), all data are presented as mean ± SEM; $^{*}p < 0.05$ vs. Sham group; ns, no significant difference vs. SAH group; $^{\#}p < 0.05$ vs. SAH + Vehicle group; $^{\&}p < 0.05$ vs. SAH + Si-NC group; $^{@}p < 0.05$ vs. SAH + Vector group; $n = 6$.

Na^+ overload, which subsequently causes Ca^{2+} entry through the reversal of Na^+/Ca^{2+} exchanger (NCX)[30,47]; and excessive cytosolic Ca^{2+} eventually leads to the occurrence of cell death[48]. Others studies have also confirmed that inhibiting NHE1 with chemical inhibitors can reduce glutamate-induced LDH release, the activity of caspase3, cellular apoptosis, and cell swelling *in vitro*[25]. However, the roles and the underlying mechanisms of NHE1 in EBI induced by SAH have not been explored.

In the present study, we confirmed that NHE1 plays an important role in EBI induced by SAH. The results of Western blot and immunofluorescence analysis suggest that NHE1 protein levels increase gradually in brain tissues after SAH, peaking at 24 h, suggesting that NHE1 may be involved in EBI induced by SAH. According to these results, we further investigated the effects of these changes in NHE1 protein levels in brain tissues on EBI. A specific chemical inhibitor of NHE1 (HOE642), genetic-knockdown and -overexpression were all applied in this research, and the results show that reduced NHE1 levels could alleviate the degree of EBI induced by SAH through decreasing the numbers of apoptotic and degenerative neurons, improving brain edema, BBB injury and neurological dysfunction, and inhibiting inflammation and oxidative stress. However, upregulation of NHE1 by genetic overexpression produces the opposite effects. Collectively, these results indicate that increased NHE1 could aggravate EBI and maybe play a negative role in the pathophysiological progression of SAH. Therefore, we further explored the underlying mechanisms of this effect. Because the activity of NHE1 can be regulated by combining with CHP1, the degree of interaction between NHE1 and CHP1 could show the activity of NHE1 in brain tissues indirectly under various treatments[27,28]. Thus, we use immunoprecipitation analysis to detect changes in the connection between NHE1 and CHP1 in brain tissues after SAH. The results show that the interaction of NHE1 and CHP1 is increased significantly in brain tissues after SAH, while it can be obviously attenuated after HOE642 and Si-NHE1

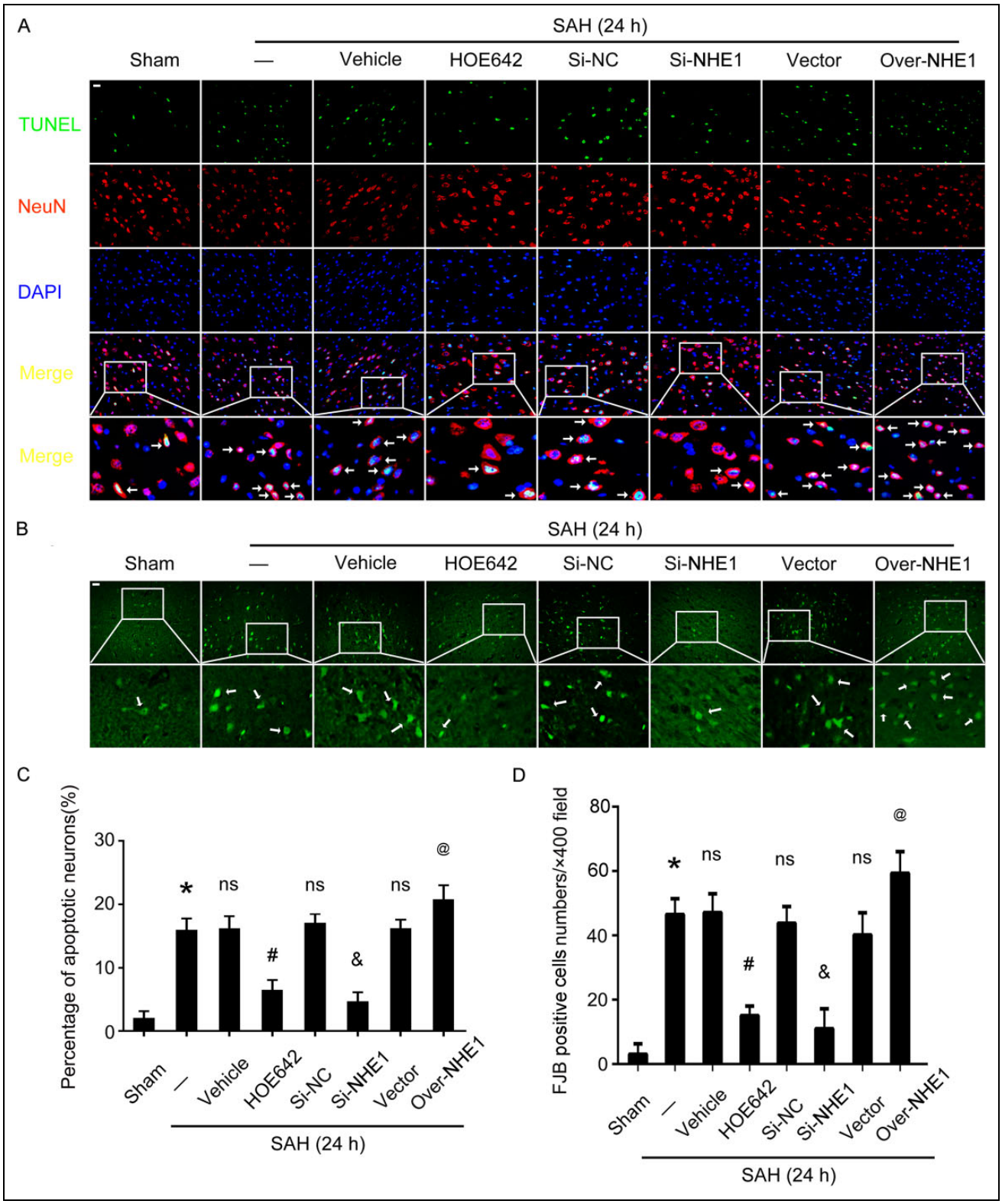

Fig. 8. Roles of NHE1 in neuronal apoptosis and degeneration in brain tissues of rats following SAH. (A) Double immunofluorescence for NeuN (red) and TUNEL (green) is performed. Nuclei is fluorescently labeled by DAPI (blue). Arrows indicate apoptotic neurons (TUNEL- and NeuN- positive cells). Scale bar = 20 μm. (B) Fluoro-Jade B (FJB) staining (green) is performed to assess neuronal degeneration in all groups at 24 h after SAH. Scale bar = 20 μm. (C) Percentages of TUNEL-positive neurons are shown. (D) Quantitative analysis of FJB positive cells in brain sections of rats in each group. FJB-positive cells are counted per ×400 field. In (B) and (D), all data are shown as mean ± SEM; $^{*}p < 0.05$ vs. Sham group; ns, no significant difference vs. SAH group; $^{\#}p < 0.05$ vs. SAH + Vehicle group; $^{\&}p < 0.05$ vs. SAH + Si-NC group; $^{@}p < 0.05$ vs. SAH + Vector group; $n = 6$.

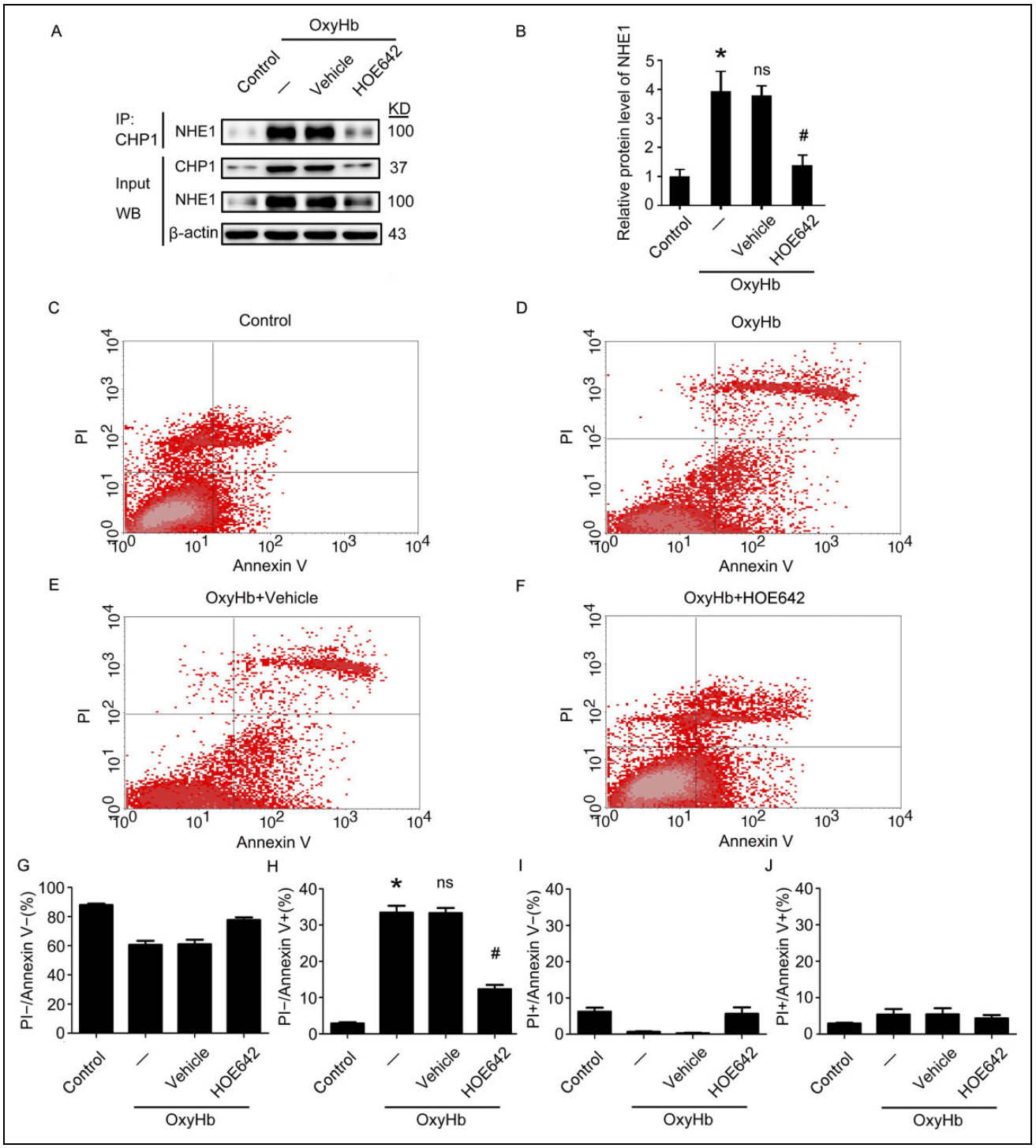

Fig. 9. Effects of inhibition NHE1 by treatment with HOE642 in OxyHb-induced neuronal apoptosis *in vitro*. (A) The interaction of NHE1 and CHP1 in cultured neurons at 24 h after OxyHb treatment is tested by immunoprecipitation (IP) analysis. Input, 5% of extract before IP. (B) Quantification of protein levels of NHE1 interacted with CHP1 in neurons at 24 h after OxyHb treatment. (C–F) PI and Annexin V double staining and flow cytometry analysis show neuronal apoptosis in various groups *in vitro*. (G–J) Bar graphs describing the different conditions of neurons in various groups. (G) PI−/Annexin V− indicates surviving neurons. (H) PI−/Annexin V+ indicates apoptotic neurons. (I) PI+/Annexin V− indicates necrotic neurons. (J) PI+/Annexin V+ exhibits a mix damage of cells. In (G)–(J), all data are presented as mean ± SEM; $^{*}p < 0.05$ vs. Control group; NS, no significant difference vs. OxyHb group; $^{\#}p < 0.05$ vs. OxyHb + Vehicle group, $n = 3$.

treatments. Taking these findings together, we can infer that combination with CHP1 is the essential molecular mechanism of NHE1 involved in EBI following SAH. Additionally, primary cultured neurons treated with OxyHb were used to mimic SAH *in vitro*, and HOE642 was applied to confirm the effect of NHE1 in neuronal apoptosis induced by OxyHb treatment *in vitro*. The results suggest that the interaction of NHE1 and CHP1 is significantly inhibited by HOE642 treatment, and the increasing ratio of neuronal apoptosis induced by OxyHb treatment is also markedly reduced under HOE642 treatment. Taken together, these results suggest that NHE1 plays an important role in neuronal apoptosis involved in EBI after SAH, and that its role may be dependent on the interaction with CHP1.

As mentioned above, NCX plays an important role in NHE1-mediated neuronal death induced by cerebral ischemia both *in vivo* and *in vitro*; whether NHE1-mediated neuronal apoptosis in brain tissues after SAH is also dependent on the activity of NCX is not clear. Additionally, the role of NHEs in BBB disruption and brain edema formation are explored in an *in vivo* study where treatment with SM-20220—a chemical NHE inhibitor—can markedly decrease brain edema and BBB damage induced by middle cerebral artery occlusion (MCAO) in a rat model[49]. Another exploration suggests that HOE642 can also reduce brain edema in a rat model of permanent MCAO[37]. Our study also shows that inhibiting NHE1 by treatment with HOE642 and application of Si-NHE1 can significantly reduce brain edema induced by SAH. Collectively, NHE1 may play an essential role in maintaining BBB functions, and its mechanisms remain in need of further investigations.

There were some limitations to this research. Firstly, only adult male rats were used to induce a SAH model *in vivo*. However, in clinical practice, we frequently find older female patients suffering from SAH. Secondly, we used primary cultured neurons merely treated with OxyHb to mimic SAH *in vitro*, but whole blood contains other relevant components, for instance heme, iron ions, plasmin, and inflammatory factors; whether these components can also induce neuronal apoptosis is not clear. Lastly, this research investigates only protein level changes and the roles of NHE1 in the EBI induced by SAH; however, the upstream signal pathways that modulate these changes and mediate these roles still remain unknown.

In conclusion, our present exploration identifies the roles of NHE1 in EBI induced by SAH. It was demonstrated that SAH induced upregulation of NHE1 protein levels in brain tissues of rats. Increased NHE1 is involved in EBI, possibly through upregulated interaction with CHP1, and led to behavioral and cognitive dysfunction, brain edema, BBB injury, inflammatory responses, oxidative stress, neuronal death, and degeneration. Meanwhile, it was confirmed that OxyHb treatment could induce an increase of combination between NHE1 and CHP1 in neurons *in vitro*, and result in neuronal death. Additionally, pharmacological inhibition and genetic knockdown of NHE1 can alleviate EBI induced by SAH through modulating the degree of combination between NHE1 and CHP1, while overexpression of NHE1 produces opposite effects. Taken these results together, we propose that NHE1 is an important regulator of neuronal death, and that it may serve as an innovative therapeutic target for SAH treatment.

Ethics Approval

All animal experimental protocols (including all use, care, and operative procedures) were approved by the Ethics Committee of the First Affiliated Hospital of Soochow University and were performed in accordance with the guidelines of the National Institutes of Health on the care and use of animals.

Statement of Human and Animal Rights

All animal experiments complied with Animal Research: Reporting of In Vivo Experiments (ARRIVE) guidelines. Every effort was made to minimize the numbers of animals used and their suffering.

Statement of Informed Consent

There were no human subjects in this article and informed consent is not applicable.

Declaration of Conflicting Interests

The author(s) declared no potential conflicts of interest with respect to the research, authorship, and/or publication of this article.

Funding

The author(s) disclosed receipt of the following financial support for the research, authorship, and/or publication of this article: This study was funded by the grant from the National Natural Science Foundation of China (No. 81571115), National Key Research and Development Program of China (No. 2018YFC1312600 and 2018YFC1312601), Project of Jiangsu Provincial Medical Innovation Team (No. CXTDA2017003), Jiangsu Provincial Medical Youth Talent (No. QNRC2016728), Suzhou Key Medical Centre (No. Szzx201501), Scientific Department of Jiangsu Province (No. BE2017656), and Suzhou Government (LCZX201601).

Supplemental Material

Supplemental material for this article is available online.

References

1. Chen S, Feng H, Sherchan P, Klebe D, Zhao G, Sun X, Zhang J, Tang J, Zhang JH. Controversies and evolving new mechanisms in subarachnoid hemorrhage. Prog Neurobiol. 2014;115:64–91.
2. Macdonald RL, Schweizer TA. Spontaneous subarachnoid haemorrhage. Lancet. 2017;389(10069):655–666.
3. Sehba FA, Hou J, Pluta RM, Zhang JH. The importance of early brain injury after subarachnoid hemorrhage. Prog Neurobiol. 2012;97(1):14–37.
4. Turan N, Heider RA, Zaharieva D, Ahmad FU, Barrow DL, Pradilla G. Sex differences in the formation of intracranial

aneurysms and incidence and outcome of subarachnoid hemorrhage: review of experimental and human studies. Transl Stroke Res. 2016;7(1):12–19.
5. Park WS, Ahn SY, Sung SI, Ahn JY, Chang YS. Mesenchymal stem cells: the magic cure for intraventricular hemorrhage? Cell Transplant. 2017;26(3):439–448.
6. Venti M. Subarachnoid and intraventricular hemorrhage. Front Neurol Neurosci. 2012;30:149–153.
7. Yamashita T, Liu W, Matsumura Y, Miyagi R, Zhai Y, Kusaki M, Hishikawa N, Ohta Y, Kim SM, Kwak TH, Han DW, Abe K. Novel therapeutic transplantation of induced neural stem cells for stroke. Cell Transplant. 2017;26(3):461–467.
8. Wu KJ, Yu S, Lee JY, Hoffer B, Wang Y. Improving neurorepair in stroke brain through endogenous neurogenesis-enhancing drugs. Cell Transplant. 2017;26(9):1596–1600.
9. Chan TM, Harn HJ, Lin HP, Chiu SC, Lin PC, Wang HI, Ho LI, Chuu CP, Chiou TW, Hsieh AC, Chen YW, Ho WY, Lin SZ. The use of ADSCs as a treatment for chronic stroke. Cell Transplant. 2014;23(4–5):541–547.
10. Gao L, Xu W, Li T, Chen J, Shao A, Yan F, Chen G. Stem cell therapy: a promising therapeutic method for intracerebral hemorrhage. Cell Transplant. 2018;27(12):1809–1824.
11. Park WS, Sung SI, Ahn SY, Sung DK, Im GH, Yoo HS, Choi SJ, Chang YS. Optimal timing of mesenchymal stem cell therapy for neonatal intraventricular hemorrhage. Cell Transplant. 2016;25(6):1131–1144.
12. Kooijman E, Nijboer CH, van Velthoven CT, Kavelaars A, Kesecioglu J, Heijnen CJ. The rodent endovascular puncture model of subarachnoid hemorrhage: mechanisms of brain damage and therapeutic strategies. J Neuroinflammation. 2014;11:2.
13. Vergouwen MD, Ilodigwe D, Macdonald RL. Cerebral infarction after subarachnoid hemorrhage contributes to poor outcome by vasospasm-dependent and -independent effects. Stroke. 2011;42(4):924–929.
14. Naidech AM, Drescher J, Tamul P, Shaibani A, Batjer HH, Alberts MJ. Acute physiological derangement is associated with early radiographic cerebral infarction after subarachnoid haemorrhage. J Neurol Neurosurg Psychiatry. 2006;77(12):1340–1344.
15. Al-Mufti F, Amuluru K, Smith B, Damodara N, El-Ghanem M, Singh IP, Dangayach N, Gandhi CD. Emerging markers of early brain injury and delayed cerebral ischemia in aneurysmal subarachnoid hemorrhage. World Neurosurg. 2017;107:148–159.
16. Serrone JC, Maekawa H, Tjahjadi M, Hernesniemi J. Aneurysmal subarachnoid hemorrhage: pathobiology, current treatment and future directions. Expert Rev Neurother. 2015;15(4):367–380.
17. Atangana E, Schneider UC, Blecharz K, Magrini S, Wagner J, Nieminen-Kelha M, Kremenetskaia I, Heppner FL, Engelhardt B, Vajkoczy P. Intravascular inflammation triggers intracerebral activated microglia and contributes to secondary brain injury after experimental subarachnoid hemorrhage (eSAH). Transl Stroke Res. 2017;8(2):144–156.
18. Xu W, Gao L, Zheng J, Li T, Shao A, Reis C, Chen S, Zhang J. The roles of MicroRNAs in stroke: possible therapeutic targets. Cell Transplant. 2018;27(12):1778–1788.
19. Munoz-Guillen NM, Leon-Lopez R, Tunez-Finana I, Cano-Sanchez A. From vasospasm to early brain injury: new frontiers in subarachnoid haemorrhage research. Neurologia. 2013;28(5):309–316.
20. Yan F, Tan X, Wan W, Dixon BJ, Fan R, Enkhjargal B, Li Q, Zhang J, Chen G, Zhang JH. ErbB4 protects against neuronal apoptosis via activation of YAP/PIK3CB signaling pathway in a rat model of subarachnoid hemorrhage. Exp Neurol. 2017;297:92–100.
21. Ji C, Chen G. Signaling pathway in early brain injury after subarachnoid hemorrhage: news update. Acta Neurochir Suppl. 2016;121:123–126.
22. Zhao H, Carney KE, Falgoust L, Pan JW, Sun D, Zhang Z. Emerging roles of Na(+)/H(+) exchangers in epilepsy and developmental brain disorders. Prog Neurobiol. 2016;138–140:19–35.
23. Packer M. Activation and inhibition of sodium-hydrogen exchanger is a mechanism that links the pathophysiology and treatment of diabetes mellitus with that of heart failure. Circulation. 2017;136(16):1548–1559.
24. Kondapalli KC, Prasad H, Rao R. An inside job: how endosomal Na(+)/H(+) exchangers link to autism and neurological disease. Front Cell Neurosci. 2014;8:172.
25. Leng T, Shi Y, Xiong ZG, Sun D. Proton-sensitive cation channels and ion exchangers in ischemic brain injury: new therapeutic targets for stroke? Prog Neurobiol. 2014;115:189–209.
26. Chang HB, Gao X, Nepomuceno R, Hu S, Sun D. Na(+)/H(+) exchanger in the regulation of platelet activation and paradoxical effects of cariporide. Exp Neurol. 2015;272:11–16.
27. Di Sole F, Vadnagara K, Moe OW, Babich V. Calcineurin homologous protein: a multifunctional Ca2+-binding protein family. Am J Physiol Renal Physiol. 2012;303(2):F165–F179.
28. Matsushita M, Tanaka H, Mitsui K, Kanazawa H. Dual functional significance of calcineurin homologous protein 1 binding to Na(+)/H(+) exchanger isoform 1. Am J Physiol Cell Physiol. 2011;301(2):C280–C288.
29. Liu Y, Zaun HC, Orlowski J, Ackerman SL. CHP1-mediated NHE1 biosynthetic maturation is required for Purkinje cell axon homeostasis. J Neurosci. 2013;33(31):12656–12669.
30. Cengiz P, Kintner DB, Chanana V, Yuan H, Akture E, Kendigelen P, Begum G, Fidan E, Uluc K, Ferrazzano P, Sun D. Sustained Na+/H+ exchanger activation promotes gliotransmitter release from reactive hippocampal astrocytes following oxygen-glucose deprivation. Plos One. 2014;9(1):e84294.
31. Wang P, Li L, Zhang Z, Kan Q, Gao F, Chen S. Time-dependent activity of Na+/H+ exchanger isoform 1 and homeostasis of intracellular pH in astrocytes exposed to CoCl2 treatment. Mol Med Rep. 2016;13(5):4443–4450.
32. Luo J, Chen H, Kintner DB, Shull GE, Sun D. Decreased neuronal death in Na+/H+ exchanger isoform 1-null mice after in vitro and in vivo ischemia. J Neurosci. 2005;25(49):11256–11268.

33. Wang Y, Luo J, Chen X, Chen H, Cramer SW, Sun D. Gene inactivation of Na+/H+ exchanger isoform 1 attenuates apoptosis and mitochondrial damage following transient focal cerebral ischemia. Eur J Neurosci. 2008;28(1):51–61.
34. Dou Y, Shen H, Feng D, Li H, Tian X, Zhang J, Wang Z, Chen G. Tumor necrosis factor receptor-associated factor 6 participates in early brain injury after subarachnoid hemorrhage in rats through inhibiting autophagy and promoting oxidative stress. J Neurochem. 2017;142(3):478–492.
35. Wang Z, Zhou F, Dou Y, Tian X, Liu C, Li H, Shen H, Chen G. Melatonin alleviates intracerebral hemorrhage-induced secondary brain injury in rats via suppressing apoptosis, inflammation, oxidative stress, DNA damage, and mitochondria injury. Transl Stroke Res. 2018;9(1):74–91.
36. Shen H, Chen Z, Wang Y, Gao A, Li H, Cui Y, Zhang L, Xu X, Wang Z, Chen G. Role of neurexin-1beta and neuroligin-1 in cognitive dysfunction after subarachnoid hemorrhage in rats. Stroke. 2015;46(9):2607–2615.
37. O'Donnell ME, Chen YJ, Lam TI, Taylor KC, Walton JH, Anderson SE. Intravenous HOE-642 reduces brain edema and Na uptake in the rat permanent middle cerebral artery occlusion model of stroke: evidence for participation of the blood-brain barrier Na/H exchanger. J Cereb Blood Flow Metab. 2013;33(2):225–234.
38. Chen CH, Chen TH, Wu MY, Chen JR, Tsai HF, Hong LY, Zheng CM, Chiu IJ, Lin YF, Hsu YH. Peroxisome proliferator-activated receptor alpha protects renal tubular cells from gentamicin-induced apoptosis via upregulating Na(+)/H(+) exchanger NHE1. Mol Med. 2015;21(1):886–899.
39. Tian X, Sun L, Feng D, Sun Q, Dou Y, Liu C, Zhou F, Li H, Shen H, Wang Z, Chen G. HMGB1 promotes neurovascular remodeling via Rage in the late phase of subarachnoid hemorrhage. Brain Res. 2017;1670:135–145.
40. Shen H, Liu C, Zhang D, Yao X, Zhang K, Li H, Chen G. Role for RIP1 in mediating necroptosis in experimental intracerebral hemorrhage model both in vivo and in vitro. Cell Death Dis. 2017;8(3):e2641.
41. Wang Z, Bu J, Yao X, Liu C, Shen H, Li X, Li H, Chen G. Phosphorylation at S153 as a functional switch of phosphatidylethanolamine binding protein 1 in cerebral ischemia-reperfusion injury in rats. Front Mol Neurosci. 2017;10:358.
42. Wang Z, Wang Y, Tian X, Shen H, Dou Y, Li H, Chen G. Transient receptor potential channel 1/4 reduces subarachnoid hemorrhage-induced early brain injury in rats via calcineurin-mediated NMDAR and NFAT dephosphorylation. Sci Rep. 2016;6:33577.
43. Yin J, Li H, Meng C, Chen D, Chen Z, Wang Y, Wang Z, Chen G. Inhibitory effects of omega-3 fatty acids on early brain injury after subarachnoid hemorrhage in rats: possible involvement of G protein-coupled receptor 120/beta-arrestin2/TGF-beta activated kinase-1 binding protein-1 signaling pathway. Int J Biochem Cell Biol. 2016;75:11–22.
44. Yuksel S, Tosun YB, Cahill J, Solaroglu I. Early brain injury following aneurysmal subarachnoid hemorrhage: emphasis on cellular apoptosis. Turk Neurosurg. 2012;22(5):529–533.
45. Chen F, Su X, Lin Z, Lin Y, Yu L, Cai J, Kang D, Hu L. Necrostatin-1 attenuates early brain injury after subarachnoid hemorrhage in rats by inhibiting necroptosis. Neuropsychiatr Dis Treat. 2017;13:1771–1782.
46. Lee JC, Cho JH, Kim IH, Ahn JH, Park JH, Cho GS, Chen BH, Shin BN, Tae HJ, Park SM, Ahn JY, Kim DW, Cho JH, Bae EJ, Yong JH, Kim YM, Won MH, Lee YL. Ischemic preconditioning inhibits expression of Na(+)/H(+) exchanger 1 (NHE1) in the gerbil hippocampal CA1 region after transient forebrain ischemia. J Neurol Sci. 2015;351(1–2):146–153.
47. Pignataro G, Sirabella R, Anzilotti S, Di Renzo G, Annunziato L. Does Na(+)/Ca(2)(+) exchanger, NCX, represent a new druggable target in stroke intervention? Transl Stroke Res. 2014;5(1):145–155.
48. Liu Q. TMBIM-mediated Ca(2+) homeostasis and cell death. Biochim Biophys Acta. 2017;1864(6):850–857.
49. Suzuki Y, Matsumoto Y, Ikeda Y, Kondo K, Ohashi N, Umemura K. SM-20220, a Na(+)/H(+) exchanger inhibitor: effects on ischemic brain damage through edema and neutrophil accumulation in a rat middle cerebral artery occlusion model. Brain Res. 2002;945(2):242–248.